AIMS Mathematics, 8(2): 3523–3541.
DOI:10.3934/math.2023179
Received: 07 October 2022
Revised: 07 November 2022
Accepted: 09 November 2022
Published: 22 November 2022

http://www.aimspress.com/journal/Math

Research articles

The global attractive sets and synchronization of a fractional-order complex dynamical system

Minghung Lin[1], Yiyou Hou[2,*], Maryam A. Al-Towailb[3] and Hassan Saberi-Nik[4,*]

[1] Department of Electrical Engineering, Cheng Shiu University, Kaohsiung 83301, Taiwan
[2] Department of Intelligent Commerce, National Kaohsiung University of Science and Technology, Kaohsiung 824004, Taiwan
[3] Department of Computer Science and Engineering, College of Applied Studies and Community Service, King Saud University, Riyadh, KSA
[4] Department of Mathematics and Statistics, University of Neyshabur, Neyshabur, Iran

* **Correspondence:** Email: yyhou@nkust.edu.tw, saberi_hssn@yahoo.com.

Abstract: This paper presents a chaotic complex system with a fractional-order derivative. The dynamical behaviors of the proposed system such as phase portraits, bifurcation diagrams, and the Lyapunov exponents are investigated. The main contribution of this effort is an implementation of Mittag-Leffler boundedness. The global attractive sets (GASs) and positive invariant sets (PISs) for the fractional chaotic complex system are derived based on the Lyapunov stability theory and the Mittag-Leffler function. Furthermore, an effective control strategy is also designed to achieve the global synchronization of two fractional chaotic systems. The corresponding boundedness is numerically verified to show the effectiveness of the theoretical analysis.

Keywords: Mittag-Leffler GAS; fractional-order complex system; Lyapunov stability theory; globally synchronization
Mathematics Subject Classification: 34A08, 34C28, 34D06, 34H10

1. Introduction

The study of the dynamical behavior of dynamical systems is attracting a lot of research efforts from various fields. The existence of chaos is an interesting phenomenon associated with a nonlinear dynamical system. Various dynamics, the existence of chaos, control, and synchronization have been studied on a large number of dynamical systems. A dynamical system involving fractional time derivatives instead of integer order time derivatives is known as a fractional dynamical system [1–6]. The fractional-order system is a generalization of an integer order system. It has been extensively

applied for the modeling of many real problems appearing in Viscoelastic systems [7], distributed-order dynamical systems [8], hydroturbine-governing systems [9], glucose-insulin regulatory systems [10] and so on.

Stability, control and synchronization are three important concepts to investigate in chaotic fractional dynamical systems. In recent years, several methods of chaos synchronization have been proposed in the literature for fractional-order chaotic systems. For example, [11] investigated optimal synchronization of chaotic fractional systems. They used finite time synchronization for an optimal control problem. The authors [12] applied function cascade synchronization for the fractional-order chaotic systems. Mahmoud et al. [13] presented the idea of complex modified projective phase synchronization of the nonlinear chaotic system with complex variables. Aghababa [14] proposed a sliding mode technique for the goal of finite-time chaos control and synchronization of fractional-order nonautonomous chaotic systems. The adaptive fuzzy control scheme, sliding-mode control, linear, nonlinear, active, feedback, and adaptive control methods have been applied for the global stability and synchronization of chaotic fractional systems [15–19].

Estimation of ultimate bound sets (UBSs) and global exponential attractive sets (GEAS) is an important topic in dynamical systems that is applied to the study of chaos control, chaos synchronization, Hausdorff dimension, and numerical search of hidden attractors [20–24]. In fact, if one can calculate an ultimate bound set (UBS) or globally attractive set (GAS) for a system, then the system cannot have chaotic attractors, equilibrium points, periodic solutions, quasi-periodic solutions, etc. outside the GAS [25, 26]. This is very important for engineering applications, since it is very difficult to predict the existence of hidden attractors. Therefore, how to get the GASs of a chaotic dynamical system is particularly significant both for theoretical research and practical applications. In 1987, Leonov published the initial results of the global UBS for the Lorenz model [27–29]. After that, Swinnerton-Dyer [30] showed that the Lyapunov function can be used to study the bounds of the states of the Lorenz equations. This idea was developed by many researchers, and they were able to compute the GAS and PIS for different chaotic systems by constructing a family of generalized Lyapunov functions including general Lorenz system [31], complex Lorenz [32], financial risk [33], chaotic dynamical finance model [34], etc.

Motivated by the above discussion, in this article, a five-dimensional fractional-order chaotic complex system is proposed. By means of theoretical analysis and numerical simulation, some basic dynamical properties, such as phase portraits, bifurcation diagram, Lyapunov exponents and chaos diagram of the presented system are studied with varying the fractional derivative orders. An interesting point that we investigated for this system is that varying the fractional-order parameter (α) causes the transition of the system from a chaotic state to a steady state. The UBS and GAS for the chaotic fractional systems have been estimated so far in two papers by Jian et al. [35, 36]. Also, Jian et al. investigated the global Mittag-Leffler boundedness for fractional-order neural networks [37, 38]. To the best of our knowledge, the GAS and the PIS for the fractional chaotic complex system have not been investigated. As an innovation, in addition to proving the global boundness of the proposed system, we calculate a family of GASs. In fact, by changing system parameters and other conditions, we can create a variety of attractive sets. The boundaries calculated for the complex chaotic system in this paper can be used for the purpose of global chaos synchronization via linear feedback controls.

This article is organized in the following sections. Section 2 presents the chaotic complex system with the fractional-order derivative. In Section 3, we will study the Mittag-Leffler GASs of the

fractional chaotic complex system. Section 4 discusses the global synchronization of two fractional chaotic systems. Conclusions are drawn in Section 5.

2. System description

In this section, we introduce a complex chaotic system with Caputo's fractional derivative. Some dynamical properties of the fractional order system, including equilibrium points, bifurcation diagrams, Lyapunov exponent spectra (LEs), and the largest Lyapunov exponent (LLE), will be presented.

2.1. The integer-order chaotic complex system

The complex chaotic system can be represented as follows [39, 40]:

$$\begin{aligned} \frac{dz_1}{dt} &= \sigma(z_2 - z_1) + z_2 z_3, \\ \frac{dz_2}{dt} &= r z_1 - z_1 z_3 - z_2, \\ \frac{dz_3}{dt} &= \frac{1}{2}(\overline{z_1} z_2 + \overline{z_2} z_1) - \beta z_3, \end{aligned} \tag{2.1}$$

where z_1 and z_2 are complex variables, $z_1 = x_1 + jx_2, z_2 = x_3 + jx_4, z_3 = x_5$, $j = \sqrt{-1}, \overline{z_1}$ and $\overline{z_2}$ are the conjugates of z_1 and z_2. The imaginary part and the real part of the complex system (2.1) are separated, which can be expressed as follows :

$$\begin{aligned} \frac{dx_1}{dt} &= \sigma(x_3 - x_1) + x_3 x_5, \\ \frac{dx_2}{dt} &= \sigma(x_4 - x_2) + x_4 x_5, \\ \frac{dx_3}{dt} &= r x_1 - x_3 - x_1 x_5, \\ \frac{dx_4}{dt} &= r x_2 - x_4 - x_2 x_5, \\ \frac{dx_5}{dt} &= x_1 x_3 + x_2 x_4 - \beta x_5. \end{aligned} \tag{2.2}$$

The authors [26, 39, 40] derived some properties of system (2.2), including Lyapunov exponents, chaotic attractor, and ultimate bound estimation.

2.2. The fractional-order chaotic complex system

The definitions of the Caputo integral and derivative are expressed in the following.

Definition 2.1. *The fractional integral function* $\mathfrak{X}(t)$*, is*

$$I^{\alpha}\mathfrak{X}(t) = \frac{1}{\Gamma(\alpha)} \int_{t_0}^{t} (t-s)^{\alpha-1} \mathfrak{X}(s) ds, \qquad t \geq t_0, \tag{2.3}$$

where $\Gamma(.)$ *is the Gamma function:*

$$\Gamma(m) = \int_0^{\infty} s^{m-1} e^{-s} ds. \tag{2.4}$$

Definition 2.2. *The Caputo fractional-order derivative of function* $\mathfrak{X} \in C^n([t_0, +\infty), \mathbb{R})$ *is*

$$D_t^{\alpha}\mathfrak{X}(t) = \frac{1}{\Gamma(n-\alpha)}\int_{t_0}^{t}(t-s)^{n-\alpha-1}\mathfrak{X}^{(n)}(s)ds. \tag{2.5}$$

Definition 2.3. *The Mittag-Leffler function* $E_{p,q}(.)$ *with two parameters is defined as*

$$E_{p,q}(m) = \sum_{k=0}^{\infty}\frac{m^k}{\Gamma(kp+q)}, \tag{2.6}$$

where $p > 0, q > 0$, *and m is a complex number. Obviously,*

$$E_p(m) = E_{p,1}(m),\ E_{0,1}(m) = \frac{1}{1-m}, E_{1,1}(m) = e^m.$$

Here, we consider the five-dimensional fractional-order system

$$\begin{aligned} D_t^{\alpha}x_1(t) &= \sigma(x_3 - x_1) + x_3x_5,\\ D_t^{\alpha}x_2(t) &= \sigma(x_4 - x_2) + x_4x_5,\\ D_t^{\alpha}x_3(t) &= rx_1 - x_3 - x_1x_5,\\ D_t^{\alpha}x_4(t) &= rx_2 - x_4 - x_2x_5,\\ D_t^{\alpha}x_5(t) &= x_1x_3 + x_2x_4 - \beta x_5, \end{aligned} \tag{2.7}$$

where σ, β, and r are parameters to be varied, and $\alpha \in (0, 1]$ is the derivative order.

The equilibrium points of the system (2.7) can be found by solving the equations

$$D_t^{\alpha}x_i = 0, (i = 1, 2, \cdots, 5).$$

After solving this equation, one can get the equilibrium points as

$$\begin{aligned} E_0 &= (0, 0, 0, 0, 0),\\ E &= (m\cos\theta, m\sin\theta, (r - \frac{rm^2}{\beta + m^2})m\cos\theta, (r - \frac{rm^2}{\beta + m^2})m\sin\theta, \frac{rm^2}{\beta + m^2}), \end{aligned}$$

where,

$$\begin{aligned} m^2 &= \frac{\beta d}{r - d},\\ d &= \frac{r - \sigma \pm \sqrt{(\sigma + r)^2 - 4\sigma}}{2}. \end{aligned}$$

When the parameters are chosen as $\sigma = 35,\ \beta = \frac{8}{3},\ r = 25$ and $\alpha = 0.98$, the system (2.7) is chaotic, as depicted in Figures 1 and 2.

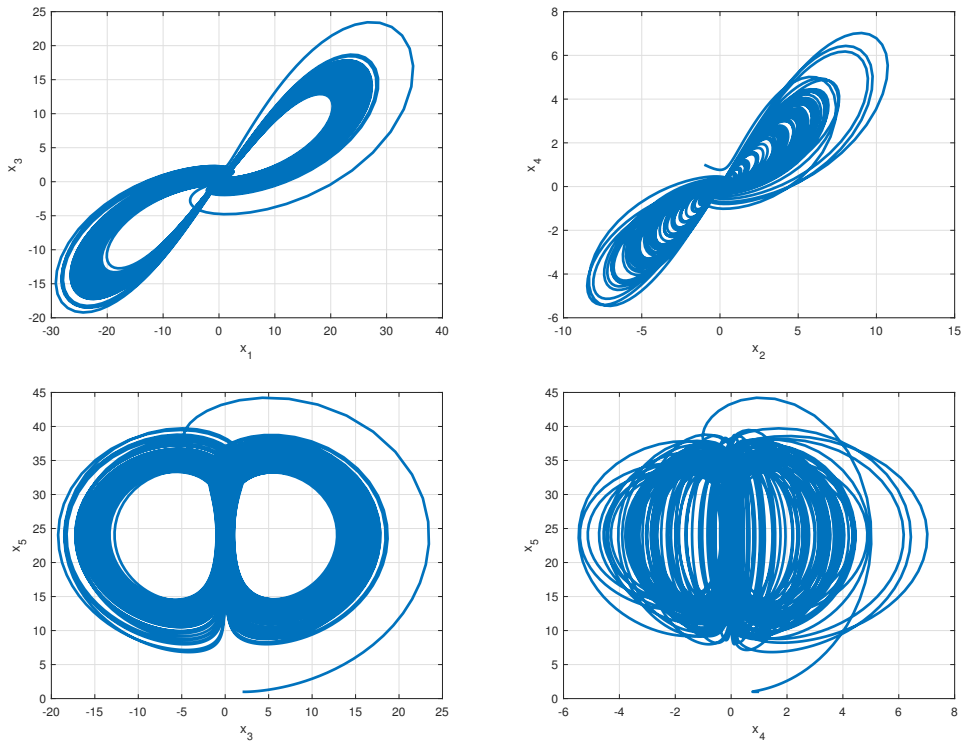

Figure 1. Phase portrait for (2.7) with $\sigma = 35, \beta = \frac{8}{3}, r = 25$ and $\alpha = 0.98$.

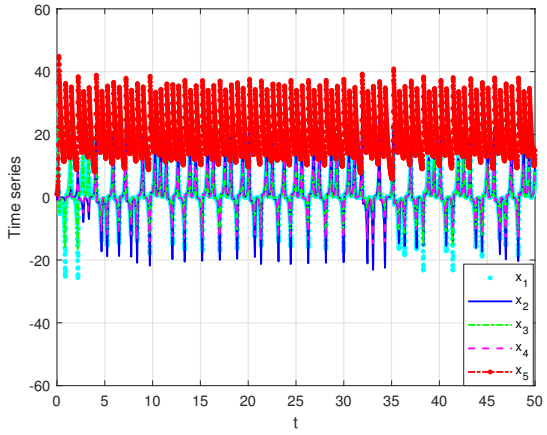

Figure 2. The chaotic behavior of system (2.7) with $\sigma = 35, \beta = \frac{8}{3}, r = 25$ and $\alpha = 0.98$.

For the fractional-order system (2.7) with $\sigma = 35, \beta = \frac{8}{3}, r = 25$ and $\alpha = 0.9$ in Figures 3 and 4, chaos is suppressed, which means the system is controlled.

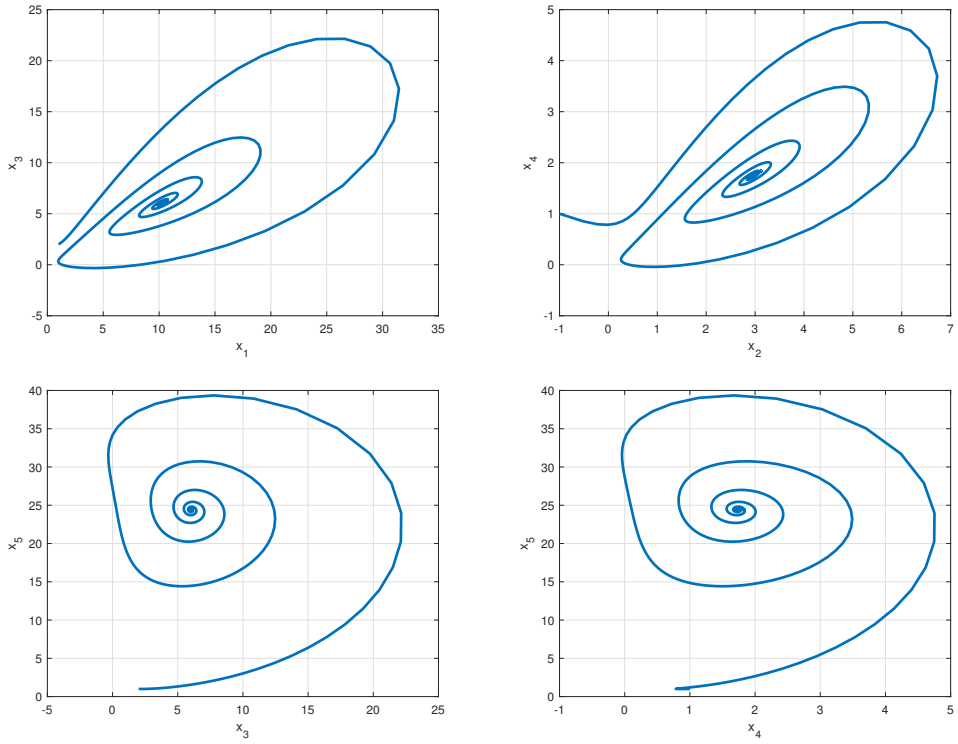

Figure 3. Phase portraitr of system (2.7) with $\sigma = 35, \beta = \frac{8}{3}, r = 25$ and $\alpha = 0.9$.

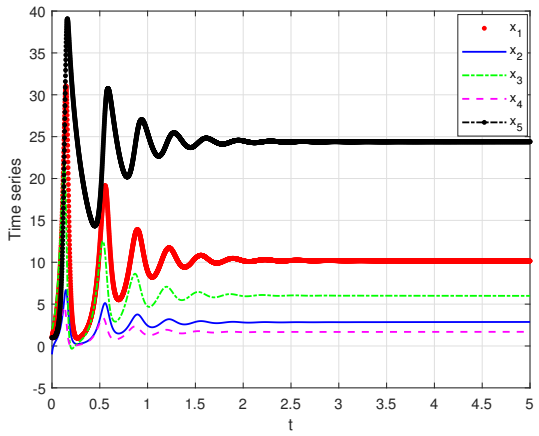

Figure 4. The behavior of system (2.7) with $\sigma = 35, \beta = \frac{8}{3}, r = 25$ and $\alpha = 0.9$.

For the values of the parameters $\sigma = 35, \beta = \frac{8}{3}$, and $r = 25$, Lyapunov exponents are shown in Figure 5. The values of Lyapunov exponents at the 500th second are $L_1 = 0.92$, $L_2 = 0.0007$, $L_3 = -0.0194$, $L_3 = -0.0194$, $L_4 = -3.5401$, $L_5 = -3.6868$.

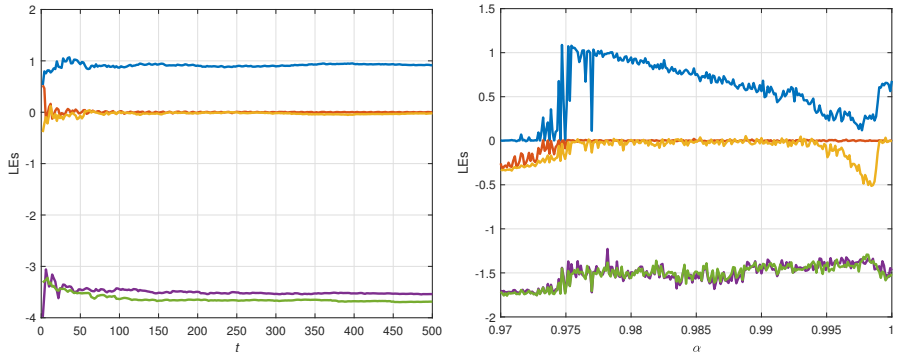

Figure 5. Lyapunov exponent spectra for system (2.7) with $\sigma = 35, \beta = \frac{8}{3}, r = 25$ and $\alpha = 0.98$.

By means of the bifurcation diagrams, Lyapunov exponent spectra (LEs) and the largest Lyapunov exponent (LLE), the dynamical properties of system (2.7) are studied. The bifurcation diagrams of the system with varying derivative orders are plotted, and the results are shown in Figure 6, where $\sigma = 35, \beta = \frac{8}{3}$, and $r = 25$. In Figure 6 derivative order α varies from 0.97 to 1 with step size of 0.005. When $\alpha < 0.972$, the system converges to a fixed point, where the LLE of the system is zero or negative. There is a periodic window when $\alpha \in (0.9941, 0.9992)$. From Figure 6, it is clearly shown that the fractional-order complex system (2.7) is chaotic over most of the scope $\alpha \in (0.97, 1)$, where the LLE of the system is positive.

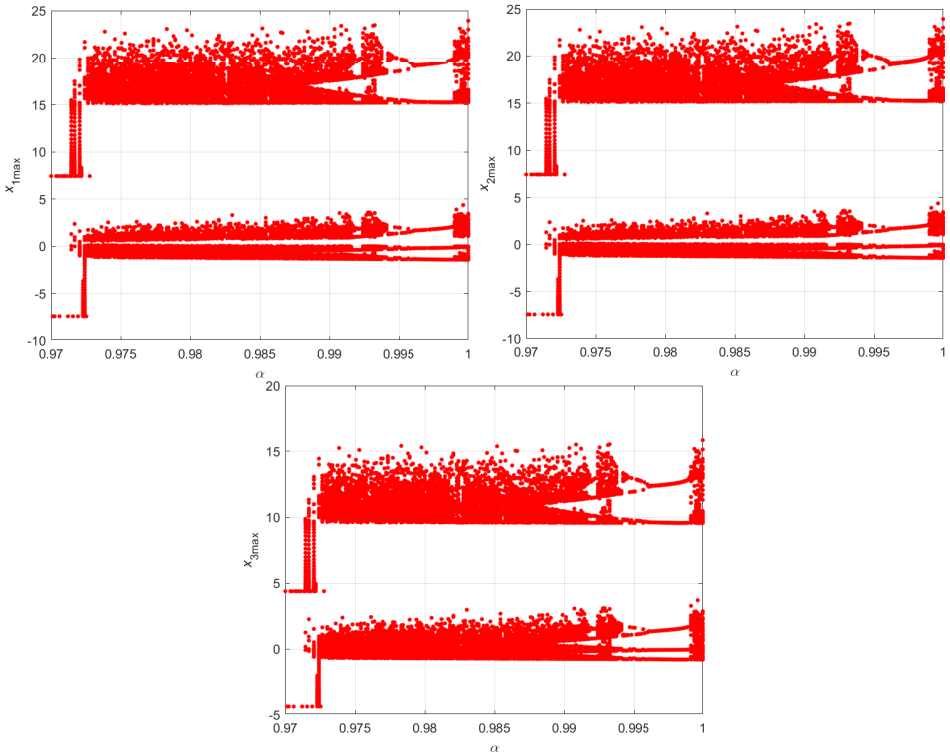

Figure 6. Bifurcation diagram obtained on variation of α, keeping the values of other parameter values, with $\sigma = 35, \beta = \frac{8}{3}, r = 25$ and $\alpha \in (0.97, 1)$.

The derivative orders can change the bifurcation types and dynamics of the system. Indeed, the derivative order is a bifurcation of the fractional-order chaotic complex system.

3. Mittag-Leffler GAS estimation of the fractional chaotic complex system

In this section, we will calculate the Mittag-Leffler GASs for the fractional-order of complex chaotic system (2.7). Let consider the following fractional-order system:

$$D_t^{\alpha}\mathfrak{X} = f(\mathfrak{X}), \quad \mathfrak{X}(t_0) = \mathfrak{X}_0, \tag{3.1}$$

where $\mathfrak{X} \in \mathbb{R}^n$, $f : \mathbb{R}^n \to \mathbb{R}^n$ is sufficiently smooth, and $\mathfrak{X}(t, t_0, \mathfrak{X}_0)$ is the solution.

Definition 3.1. *[35] For a given Lyapunov function $\mathcal{V}_\lambda(t) = \mathcal{V}_\lambda(\mathfrak{X}(t))$ with $\lambda > 0$, if there exist constants $\mathcal{L}_\lambda > 0$ and $r_\lambda > 0$ for all $\mathfrak{X}_0 \in \mathbb{R}^n$ such that*

$$\mathcal{V}_\lambda(t) - \mathcal{L}_\lambda \leq (\mathcal{V}_\lambda(t_0) - \mathcal{L}_\lambda)E_\alpha(-r_\lambda(t - t_0)^\alpha), \ \ t \geq t_0, \tag{3.2}$$

for $\mathcal{V}_\lambda(\mathfrak{X}) > \mathcal{L}_\lambda$, then $\mathcal{U}_\lambda = \{\mathfrak{X}|\mathcal{V}_\lambda(\mathfrak{X}(t)) \leq \mathcal{L}_\lambda\}$ is said to be the Mittag-Leffler GAS of system (3.1). If for any $\mathfrak{X}_0 \in \mathcal{U}_\lambda$ and any $t > t_0$, $\mathfrak{X}(t, t_0, \mathfrak{X}_0) \in \mathcal{U}_\lambda$, then $\mathcal{U}_\lambda$ is said to be a Mittag-Leffler PISs, where $\mathfrak{X} = \mathfrak{X}(t), \mathfrak{X}_0 = \mathfrak{X}(t_0)$.

Lemma 3.1. *[36] If $\mathfrak{X}(t) \in \mathbb{R}$ is a continuous and differentiable function, then*

$$D^\alpha(\mathfrak{X}^2(t)) \leq 2\mathfrak{X}(t)D^\alpha(\mathfrak{X}(t)). \tag{3.3}$$

Lemma 3.2. *[36] For $\alpha \in (0, 1)$ and constant $\kappa \in \mathbb{R}$, if a continuous function $\mathfrak{X}(t)$ meets*

$$D^\alpha(\mathfrak{X}(t)) \leq \kappa\mathfrak{X}(t), \quad t \geq 0, \tag{3.4}$$

then

$$\mathfrak{X}(t) \leq \mathfrak{X}(0)E_\alpha(\kappa t^\alpha), \quad t \geq 0. \tag{3.5}$$

The following theorem investigated the Mittag-Leffler GASs and the Mittag-Leffler PISs of the system (2.7):

Theorem 3.1. *Let $\beta > 0, \sigma > 0$ and $r > 0$. Define*

$$\mathcal{U}_{\lambda,\mu} = \left\{ X(t) \in \mathbb{R}^5 \mid \lambda x_1^2 + \lambda x_2^2 + (\lambda + \mu)x_3^2 + (\lambda + \mu)x_4^2 + \mu\left(x_5 - \frac{(\sigma + r)\lambda + r\mu}{\mu}\right)^2 \leq R_{max}^2 \right\}. \tag{3.6}$$

Then, $\mathcal{U}_{\lambda,\mu}$ is the ultimate bound and positively invariant set of system (2.7), where

$$R_{max}^2 = \frac{\beta((\sigma + r)\lambda + r\mu)^2}{\eta\mu} \tag{3.7}$$

and $\eta = min\{1, \sigma, \beta\} > 0$.

Proof. Define the following generalized positively definite and radically unbounded Lyapunov function

$$V_{\lambda,\mu}(x_1, x_2, x_3, x_4, x_5) = \frac{1}{2}\lambda x_1^2 + \frac{1}{2}\lambda x_2^2 + \frac{1}{2}(\lambda+\mu)x_3^2 + \frac{1}{2}(\lambda+\mu)x_4^2 + \frac{1}{2}\mu\left(x_5 - \frac{(\sigma+r)\lambda + r\mu}{\mu}\right)^2, \tag{3.8}$$

where $\lambda > 0, \mu > 0$.
Computing the fractional derivative of $V_{\lambda,\mu}$ along the trajectory of system (2.7) and using Lemma 3.1, we have

$$\begin{aligned}
D_t^\alpha V_{\lambda,\mu}(X(t)) &\le \lambda x_1 D_t^\alpha x_1 + \lambda x_2 D^\alpha x_2 + (\lambda+\mu)x_3 D_t^\alpha x_3 \\
&\quad + (\lambda+\mu)x_4 D_t^\alpha x_4 + \mu\left(x_5 - \frac{(\sigma+r)\lambda + r\mu}{\mu}\right) D_t^\alpha x_5 \\
&= \lambda x_1\left(\sigma(x_3 - x_1) + x_3 x_5\right) + \lambda x_2(\sigma(x_4 - x_2) + x_4 x_5) \\
&\quad + (\lambda+\mu)x_3(r x_1 - x_3 - x_1 x_5) + (\lambda+\mu)x_4(r x_2 - x_4 - x_2 x_5) \\
&\quad + \mu\left(x_5 - \frac{(\sigma+r)\lambda + r\mu}{\mu}\right)(x_1 x_3 + x_2 x_4 - \beta x_5) \\
&= -\lambda\sigma x_1^2 - \lambda\sigma x_2^2 - (\lambda+\mu)x_3^2 - (\lambda+\mu)x_4^2 - \mu\beta x_5^2 + \beta((\sigma+r)\lambda + r\mu)x_5 \\
&= -\frac{1}{2}\lambda\sigma x_1^2 - \frac{1}{2}\lambda\sigma x_2^2 - \frac{1}{2}(\lambda+\mu)x_3^2 - \frac{1}{2}(\lambda+\mu)x_4^2 - \frac{1}{2}\mu\beta\left(x_5 - \frac{(\sigma+r)\lambda + r\mu}{\mu}\right)^2 + F(X),
\end{aligned}$$

where,

$$F(X) = -\frac{1}{2}\lambda\sigma x_1^2 - \frac{1}{2}\lambda\sigma x_2^2 - \frac{1}{2}(\lambda+\mu)x_3^2 - \frac{1}{2}(\lambda+\mu)x_4^2 - \frac{1}{2}\mu\beta x_5^2 + \frac{\beta((\sigma+r)\lambda + r\mu)^2}{2\mu}. \tag{3.9}$$

It is obvious that $F(X) \le \sup_{X\in\mathbb{R}^5} F(X) = l_{\lambda,\mu} = \dfrac{\beta((\sigma+r)\lambda + r\mu)^2}{2\mu}$. From there we have

$$D_t^\alpha V_{\lambda,\mu}(X(t)) \le -\eta V_{\lambda,\mu} + l_{\lambda,\mu}, \tag{3.10}$$

i.e.,

$$D_t^\alpha(V_{\lambda,\mu}(t) - \frac{l_{\lambda,\mu}}{\eta}) \le -\eta(V_{\lambda,\mu}(t) - \frac{l_{\lambda,\mu}}{\eta}). \tag{3.11}$$

Based on Lemma 3.2 , one can obtain

$$V_{\lambda,\mu}(t) - \frac{l_{\lambda,\mu}}{\eta} \le (V_{\lambda,\mu}(0) - \frac{l_{\lambda,\mu}}{\eta})E_\alpha(-\eta t^\alpha),\ t \ge 0. \tag{3.12}$$

Based on Definition 3.1, from (3.12) we conclude that the ellipsoid $\mathcal{U}_{\lambda,\mu}$ for $\beta > 0, \sigma > 0$ and $r > 0$ is a Mittag-Leffler GAS and Mittag-Leffler PIS for the system (2.7). This completes the proof. □

By changing the values of λ and μ, we can achieve different bounded sets. An interesting property about the the fractional-order parameter is that the change of α leads to a change in the behavior of the dynamical system from a chaotic state to a steady state.

(i) If we take $\lambda = 1, \mu = 1$, then

$$\mathcal{U}_{1,1} = \left\{(x_1, x_2, x_3, x_4, x_5) | x_1^2 + x_2^2 + 2x_3^2 + 2x_4^2 + (x_5 - (\sigma + 2r))^2 \leq \beta(\sigma + 2r)^2\right\},$$

is the Mittag-Leffler GAS of system (2.7).

When $\sigma = 35, b = \frac{8}{3}$, and $r = 25$, we have

$$\mathcal{U}_{1,1} = \left\{(x_1, x_2, x_3, x_4, x_5) | x_1^2 + x_2^2 + 2x_3^2 + 2x_4^2 + (x_5 - 85)^2 \leq (138.8)^2\right\}.$$

Figure 7 shows the chaotic attractors and the Mittag-Leffler GASs of the system (2.7) in the different spaces defined by $\mathcal{U}_{1,1}$, for $\sigma = 35, \beta = \frac{8}{3}, r = 25$, and $\alpha = 0.98$. Considering the value of $\alpha = 0.95$, the solutions of (2.7) change from chaotic to steady-state. In this case, we found that chaos does not exist in the nonlinear fractional-order model. The phase portraits and Mittag-Leffler GAS of system (2.7) are shown through Figure 8.

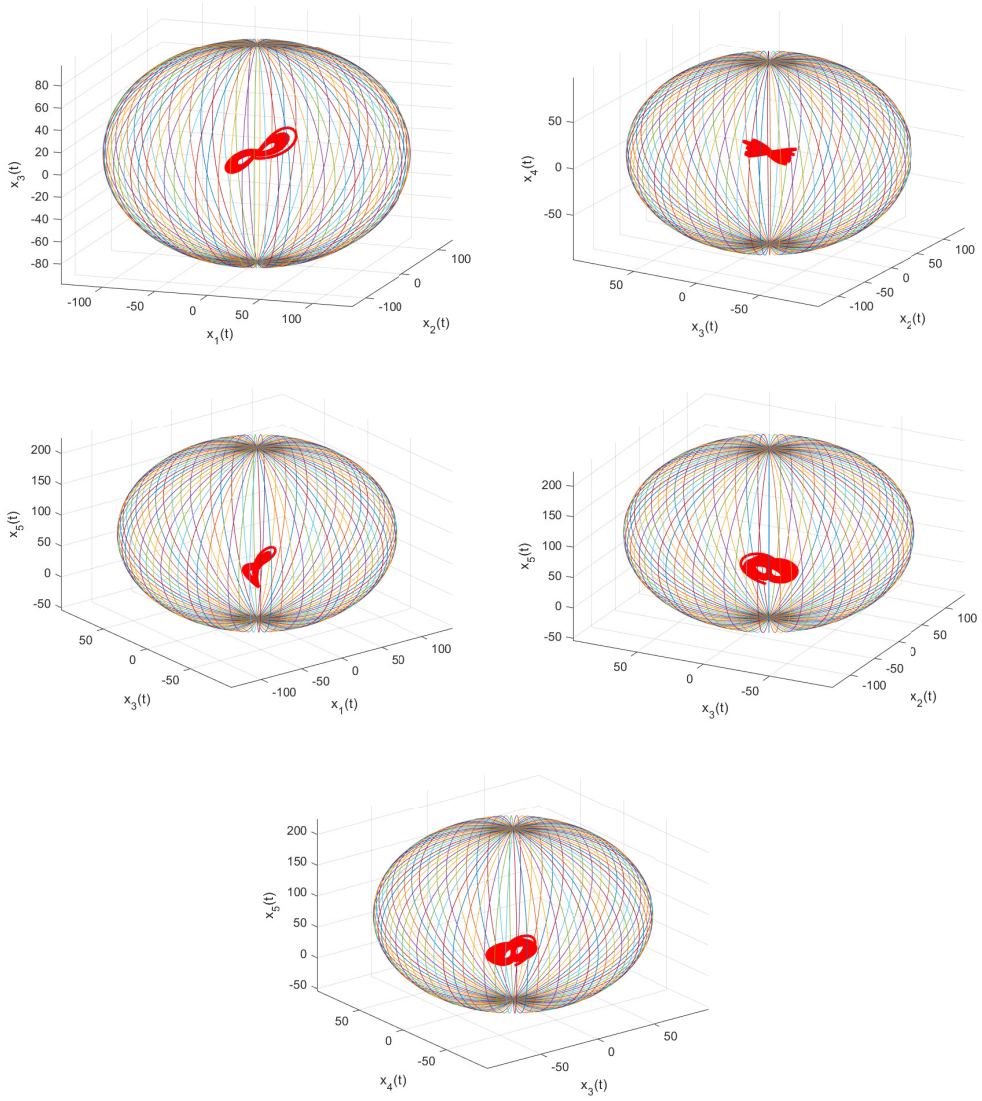

Figure 7. Mittag-Leffler GAS of the system (2.7) with $\sigma = 35, \beta = \frac{8}{3}, r = 25$, and $\alpha = 0.98$.

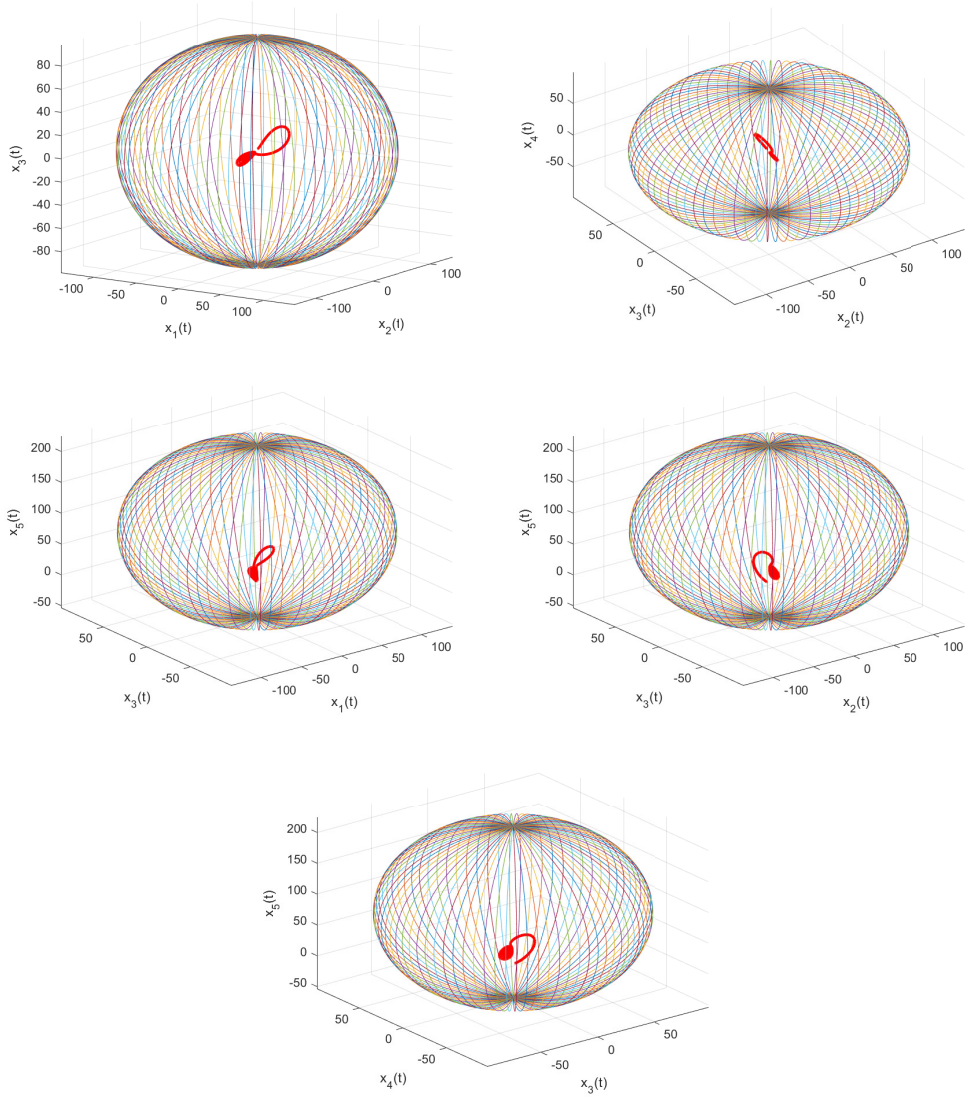

Figure 8. Mittag-Leffler GAS of the system (2.7) with $\sigma = 35, \beta = \frac{8}{3}, r = 25$, and $\alpha = 0.95$.

(ii) Let us take $\lambda = 1, \mu = 2$, and then we get that the set

$$\mathcal{U}_{1,2} = \left\{(x_1, x_2, x_3, x_4, x_5)|x_1^2 + x_2^2 + 3x_3^2 + 3x_4^2 + 2(x_5 - \frac{\sigma + 3r}{2})^2 \leq \frac{\beta(\sigma + 3r)^2}{2}\right\},$$

is the Mittag-Leffler GAS of system (2.7).

When $\sigma = 35, b = \frac{8}{3}$, and $r = 25$, we have

$$\mathcal{U}_{1,2} = \left\{(x_1, x_2, x_3, x_4, x_5)|x_1^2 + x_2^2 + 3x_3^2 + 3x_4^2 + 2(x_5 - 55)^2 \leq 127.01^2\right\}.$$

Figure 9 shows the phase portraits and the Mittag-Leffler GAS of system (2.7) in the different spaces defined by $\mathcal{U}_{1,2}$.

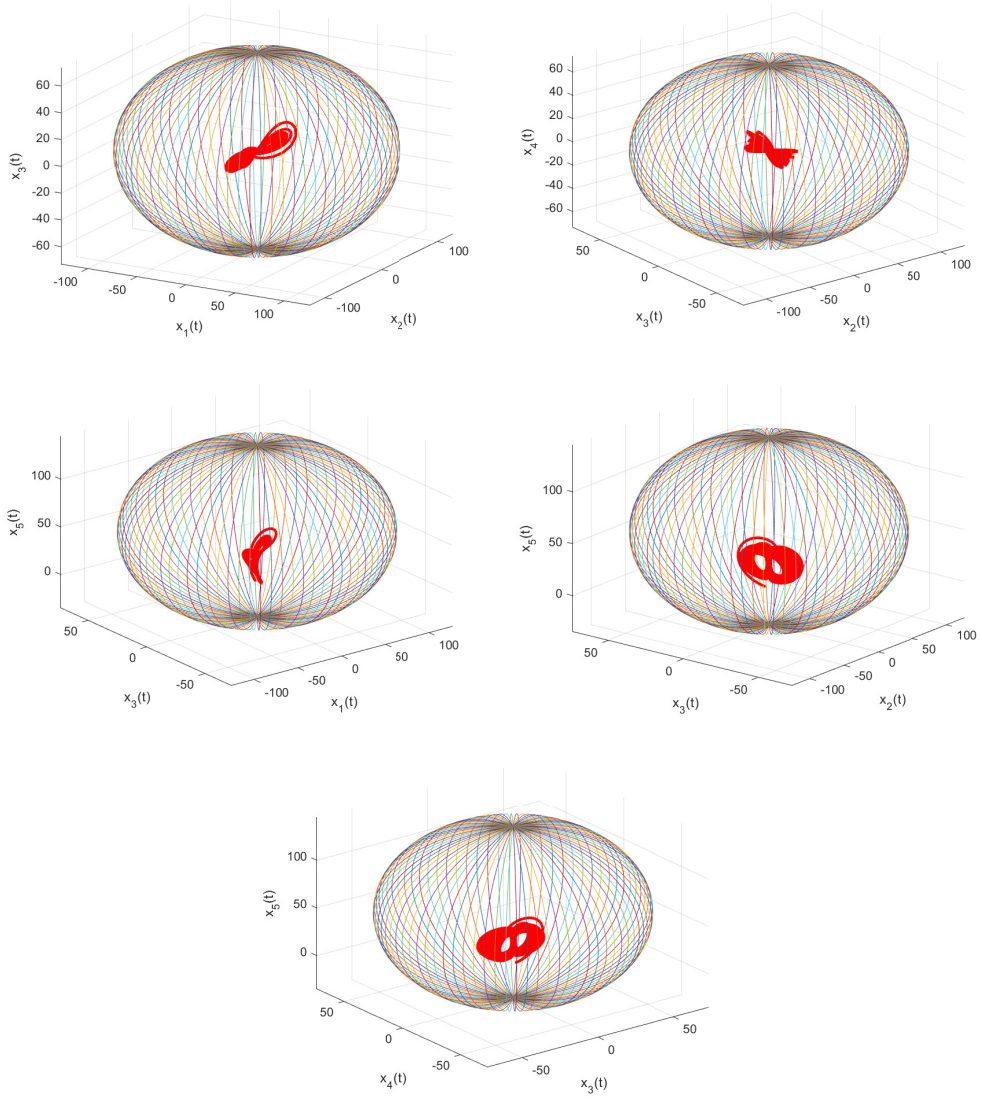

Figure 9. Mittag-Leffler GAS of the system (2.7) with $\sigma = 35, \beta = \frac{8}{3}, r = 25$, and $\alpha = 0.98$.

(iii) Let us take $\lambda = 2, \mu = 1$, and then we get that the set

$$\mathcal{U}_{2,1} = \left\{(x_1, x_2, x_3, x_4, x_5) | 2x_1^2 + x_2^2 + 3x_3^2 + 3x_4^2 + (x_5 - (2\sigma + 3r))^2 \leq \beta(2\sigma + 3r)^2\right\},$$

is the Mittag-Leffler GAS of system (2.7).

When $\sigma = 35, b = \frac{8}{3}, r = 25$, and $\alpha = 0.98$, we have

$$\mathcal{U}_{2,1} = \left\{(x_1, x_2, x_3, x_4, x_5) | 2x_1^2 + 2x_2^2 + 3x_3^2 + 3x_4^2 + (x_5 - 145)^2 \leq 236.7^2\right\}.$$

4. Global synchronization via linear feedback

In this section, we study the global synchronization of the complex chaotic system via linear feedback control. Let us state the following two lemmas which are used to prove synchronization in the presented system.

Lemma 4.1. *[32] For any $\epsilon > 0, \mathfrak{a} \in \mathbb{R}, \mathfrak{b} \in \mathbb{R}$, the inequality $2\mathfrak{a}\mathfrak{b} \leq \epsilon\mathfrak{a}^2 + \frac{1}{\epsilon}\mathfrak{b}^2$ holds.*

Lemma 4.2. *[32] For $k > 0, \mathfrak{a} \in \mathbb{R}$ and $\mathfrak{b} \in \mathbb{R}$, the inequality $-k\mathfrak{a}^2 + \mathfrak{a}\mathfrak{b} \leq -\frac{1}{2}k\mathfrak{a}^2 + \frac{1}{2k}\mathfrak{b}^2$ holds.*

Let system (2.7) be the drive system with the response system

$$\begin{aligned} D_t^\alpha y_1(t) &= \sigma(y_3 - y_1) + y_3y_5 + u_1, \\ D_t^\alpha y_2(t) &= \sigma(y_4 - y_2) + y_4y_5 + u_2, \\ D_t^\alpha y_3(t) &= ry_1 - y_3 - y_1y_5 + u_3, \\ D_t^\alpha y_4(t) &= ry_2 - y_4 - y_2y_5 + u_4, \\ D_t^\alpha y_5(t) &= y_1y_3 + y_2y_4 - \beta y_5 + u_5, \end{aligned} \tag{4.1}$$

where $y_1, y_2, \cdots, y_5$ are state variables and $u_1, u_2, \cdots, u_5$ are controllers to be designed so as to achieve global chaos synchronization between systems (4.1) and (2.7). From (3.6) in Theorem 3.1, we have

$$|x_1| \leq \frac{R_{max}}{\sqrt{\lambda}}, \ \ |x_2| \leq \frac{R_{max}}{\sqrt{\lambda}}, \ \ |x_3| \leq \frac{R_{max}}{\sqrt{\lambda+\mu}}, \ \ |x_4| \leq \frac{R_{max}}{\sqrt{\lambda+\mu}}, \ \ |x_5 - \theta| \leq \frac{R_{max}}{\sqrt{\mu}}.$$

Therefore, we can get the maximum boundness of states as the following:

$$\begin{aligned} M_1 &= \frac{R_{max}}{\sqrt{\lambda}}, \\ M_2 &= \frac{R_{max}}{\sqrt{\lambda}}, \\ M_3 &= \frac{R_{max}}{\sqrt{\lambda+\mu}}, \\ M_4 &= \frac{R_{max}}{\sqrt{\lambda+\mu}}, \\ M_5 &= \frac{R_{max}}{\sqrt{\mu}} + \theta, \end{aligned}$$

where $\theta = \frac{(\sigma+r)\lambda+r\mu}{\mu}$. Then, we have the following theorem.

Theorem 4.1. *The global synchronization between the drive system (2.7) and response system (4.1) will occur via the control laws*

$$u_1 = u_2 = u_5 = 0, \ \ u_3 = -k_3e_3, \ \ u_4 = -k_4e_4, \tag{4.2}$$

where

$k_3 > \frac{\sigma+2r+M_5}{2\epsilon} + \frac{M_1}{2} - 2, \quad k_4 > \frac{\sigma+2r+M_5}{2\epsilon} + \frac{M_2}{2} - 2, \quad 0 < \epsilon < \frac{\sigma}{\sigma+2r+M_5+\theta}.$

Proof. Let the state errors be $e_i = y_i - x_i, i = 1, 2, \cdots, 5$. By subtracting (2.7) from (4.1), we obtain the error dynamical system:

$$D_t^\alpha e_1(t) = \sigma(e_3 - e_1) + e_3e_5 + e_3x_5 + e_5x_3,$$

$$\begin{aligned} D_t^\alpha e_2(t) &= \sigma(e_4 - e_2) + e_4e_5 + e_4x_5 + e_5x_4, \\ D_t^\alpha e_3(t) &= re_1 - e_3 - e_1e_5 - e_1x_5 - e_5x_1 - k_3e_3, \\ D_t^\alpha e_4(t) &= re_2 - e_4 - e_2e_5 - e_2x_5 - e_5x_2 - k_4e_4, \\ D_t^\alpha e_5(t) &= e_1e_3 + e_1x_3 + e_3x_1 + e_2e_4 + e_2x_4 + e_4x_2 - \beta e_5. \end{aligned} \tag{4.3}$$

Let $V(e) = \frac{1}{2}e_1^2 + \frac{1}{2}e_2^2 + e_3^2 + e_4^2 + \frac{1}{2}e_5^2$. Based on Lemma 3.1, the fractional-order derivative of V along the system (4.3) is

$$\begin{aligned} D_t^\alpha V(e) &\le e_1D_t^\alpha e_1 + e_2D_t^\alpha e_2 + 2e_3D_t^\alpha e_3 + 2e_4D_t^\alpha e_4 + e_5D_t^\alpha e_5 \\ &= e_1(\sigma(e_3 - e_1) + e_3e_5 + e_3x_5 + e_5x_3) + e_2(\sigma(e_4 - e_2) + e_4e_5 + e_4x_5 + e_5x_4) \\ &+ 2e_3(re_1 - e_3 - e_1e_5 - e_1x_5 - e_5x_1 - k_3e_3) + 2e_4(re_2 - e_4 - e_2e_5 - e_2x_5 - e_5x_2 - k_4e_4) \\ &+ e_5(e_1e_3 + e_1x_3 + e_3x_1 + e_2e_4 + e_2x_4 + e_4x_2 - \beta e_5) \\ &= -\sigma e_1^2 - \sigma e_2^2 - (2 + k_3)e_3^2 - (2 + k_4)e_4^2 - \beta e_5^2 \\ &+ (\sigma + 2r)e_1e_3 + (\sigma + 2r)e_2e_4 + 2e_1e_5x_3 + 2e_2e_5x_4 - e_3e_5x_1 - e_4e_5x_2 - e_2e_4x_5 - e_1e_3x_5. \end{aligned}$$

From Lemmas 4.1 and 4.2, we have

$$\begin{aligned} &(\sigma + 2r - x_5)e_1e_3 \le (\sigma + 2r + M_5 + \theta)|e_1||e_3| \le \frac{\epsilon}{2}(\sigma + 2r + M_5 + \theta)e_1^2 + \frac{1}{2\epsilon}(\sigma + 2r + M_5 + \theta)e_3^2, \\ &(\sigma + 2r - x_5)e_2e_4 \le (\sigma + 2r + M_5 + \theta)|e_2||e_4| \le \frac{\epsilon}{2}(\sigma + 2r + M_5 + \theta)e_2^2 + \frac{1}{2\epsilon}(\sigma + 2r + M_5 + \theta)e_4^2, \\ &-\sigma e_1^2 + 2e_1e_5x_3 \le -\sigma e_1^2 + 2M_3|e_1||e_5| \le -\frac{1}{2}\sigma e_1^2 + \frac{2}{\sigma}M_3^2e_5^2, \\ &-\sigma e_2^2 + 2e_2e_5x_4 \le -\sigma e_2^2 + 2M_4|e_2||e_5| \le -\frac{1}{2}\sigma e_2^2 + \frac{2}{\sigma}M_4^2e_5^2, \\ &-e_4e_5x_2 - e_3e_5x_1 \le M_2|e_4||e_5| + M_1|e_3||e_5| \le \frac{M_2}{2}(e_4^2 + e_5^2) + \frac{M_1}{2}(e_3^2 + e_5^2). \end{aligned}$$

Then,

$$\begin{aligned} D_t^\alpha V(e) \le &-\frac{1}{2}(\sigma - \sigma\epsilon - 2r\epsilon - \epsilon M_5 - \epsilon\theta)e_1^2 - \frac{1}{2}(\sigma - \sigma\epsilon - 2r\epsilon - \epsilon M_5 - \epsilon\theta)e_2^2 \\ &- (2 + k_3 - \frac{\sigma + 2r + M_5}{2\epsilon} - \frac{M_1}{2})e_3^2 - (2 + k_4 - \frac{\sigma + 2r + M_5}{2\epsilon} - \frac{M_2}{2})e_4^2 \\ &- \frac{1}{2}(2\beta - \frac{4}{\sigma}M_3^2 - \frac{4}{\sigma}M_4^2 - M_1 - M_2)e_5^2. \end{aligned}$$

Set

$$\begin{aligned} &\eta_1 = \sigma - \sigma\epsilon - 2r\epsilon - \epsilon M_5 - \epsilon\theta, \ \ \eta_2 = \sigma - \sigma\epsilon - 2r\epsilon - \epsilon M_5 - \epsilon\theta, \ \ \eta_3 = 2 + k_3 - \frac{\sigma + 2r + M_5}{2\epsilon} - \frac{M_1}{2}, \\ &\eta_4 = 2 + k_4 - \frac{\sigma + 2r + M_5}{2\epsilon} - \frac{M_2}{2}, \ \ \eta_5 = 2\beta - \frac{4}{\sigma}M_3^2 - \frac{4}{\sigma}M_4^2 - M_1 - M_2. \end{aligned}$$

Then, $D_t^\alpha V(e) \le -\eta V$, where $\eta = \min\{\eta_1, \eta_2, \eta_3, \eta_4, \eta_5\}$. By Lemma 3.2, one can obtain $V(t) \le V(0)E_\alpha(-\eta t^\alpha)$, $t \ge 0$; and thus the error system (4.3) is global stable at $e = 0$, implying the global

Mittag-Leffler synchronization of trajectories in fractional-order systems (2.7) and (4.1) by control laws (4.2).

To check the correctness of the presented theory for synchronization, we used simulation using MATLAB version 2021. The parameters of both systems are taken as $\sigma = 35, \beta = \frac{8}{3}, r = 43$, and $\alpha = 0.98$. The initial values of the master and slave systems are $(1, -1, 2, 1, 1)$ and $(0, 0.1, -1, 0, 0)$. Controllers (4.2) with $k_3 = 150$, (4.2) and $k_4 = 160$, are chosen, and then response system (4.1) synchronizes with drive system (2.7), as shown in Figures 10. Figure 11, shows synchronization errors between systems (2.7) and (4.1). From these figures, it is evident that the response trajectories fully converge to the drive, and the synchronization errors $e_i = y_i - x_i$ for $i = 1, 2, 3, 4, 5$ converge to zero.

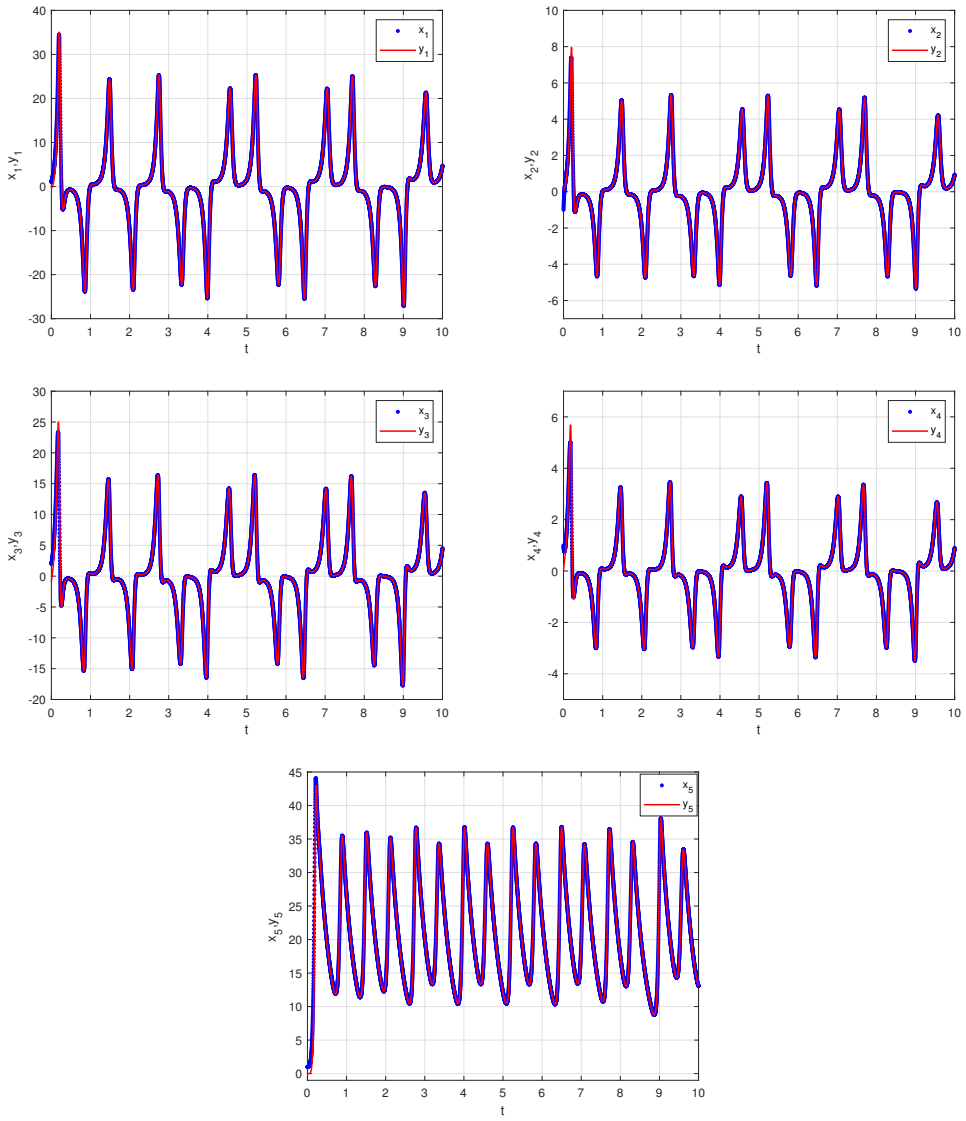

Figure 10. State trajectories of the drive-response systems for the fractional-order chaotic complex system.

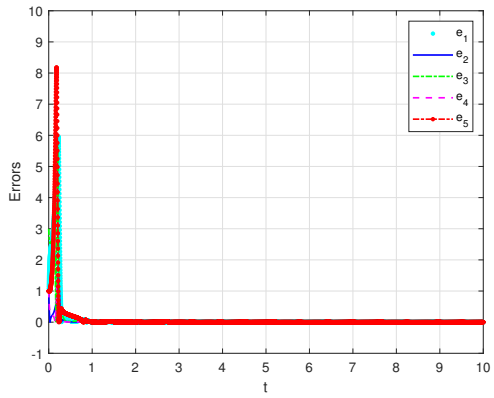

Figure 11. The synchronization errors of fractional-order chaotic complex system.

□

5. Conclusions

In this paper, we introduced the fractional-order chaotic complex system. Using the Lyapunov function and fractional-order derivative, the Mittag-Leffler GASs and Mittag-Leffler PISs for this system are obtained. Furthermore, we investigated some dynamical properties of the system, including phase portraits, bifurcation diagrams, and the Lyapunov exponents. Finally, based on the Lyapunov theory, we designed a linear feedback control to synchronize the two chaotic complex systems. Simulation results are given to show the validity of the proposed schemes.

Acknowledgments

This work was supported by the National Science and Technology Council of Republic of China under contract NSTC 111-2622-B-214-001.

Conflict of interest

The authors declare that there is no conflict of interests regarding the publication of this article.

References

1. A. Dlamini, E. Doungmo Goufo, M. Khumalo, On the Caputo-Fabrizio fractal fractional representation for the Lorenz chaotic system, *AIMS Mathematics*, **6** (2021), 12395–12421. http://dx.doi.org/10.3934/math.2021717
2. S. David, J. Machado, D. Quintino, J. Balthazar, Partial chaos suppression in a fractional-order macroeconomic model, *Math. Comput. Simulat.*, **122** (2016), 55–68. http://dx.doi.org/10.1016/j.matcom.2015.11.004
3. E. Bonyah, Chaos in a 5-D hyperchaotic system with four wings in the light of non-local and non-singular fractional derivatives, *Chaos Soliton. Fract.*, **116** (2018), 316–331. http://dx.doi.org/10.1016/j.chaos.2018.09.034

4. E. Mahmoud, P. Trikha, L. Jahanzaib, O. Almaghrabi, Dynamical analysis and chaos control of the fractional chaotic ecological model, *Chaos Soliton. Fract.*, **141** (2020), 110348. http://dx.doi.org/10.1016/j.chaos.2020.110348

5. V. Pham, S. Kingni, C. Volos, S. Jafari, T. Kapitaniak, A simple three-dimensional fractional-order chaotic system without equilibrium: dynamics, circuitry implementation, chaos control and synchronization, *AEU-Int. J. Electron. C.*, **78** (2017), 220–227. http://dx.doi.org/10.1016/j.aeue.2017.04.012

6. Y. He, J. Peng, S. Zheng, Fractional-order financial system and fixed-time synchronization, *Fractal Fract.*, **6** (2022), 507. http://dx.doi.org/10.3390/fractalfract6090507

7. Y. Xu, Y. Li, D. Liu, Response of fractional oscillators with viscoelastic term under random excitation, *J. Comput. Nonlinear Dyn.*, **9** (2014), 031015. http://dx.doi.org/10.1115/1.4026068

8. Z. Jiao, Y. Chen, I. Podlubny, *Distributed-order dynamic systems*, London: Springer, 2012. http://dx.doi.org/10.1007/978-1-4471-2852-6

9. B. Xu, D. Chen, H. Zhang, F. Wang, Modeling and stability analysis of a fractional-order Francis hydro-turbine governing system, *Chaos Soliton. Fract.*, **75** (2015), 50–61. http://dx.doi.org/10.1016/j.chaos.2015.01.025

10. K. Rajagopal, A. Bayani, S. Jafari, A. Karthikeyan, I. Hussain, Chaotic dynamics of a fractional-order glucoseinsulin regulatory system, *Front. Inform. Technol. Electron. Eng.*, **21** (2020), 1108–1118. http://dx.doi.org/10.1631/FITEE.1900104

11. M. Farmani Ardehaei, M. Farahi, S. Effati, Finite time synchronization of fractional chaotic systems with several slaves in an optimal manner, *Phys. Scr.*, **95** (2020), 035219. http://dx.doi.org/10.1088/1402-4896/ab474d

12. H. An, D. Feng, L. Sun, H. Zhu, The fractional-order unified chaotic system: A general cascade synchronization method and application, *AIMS Mathematics*, **5** (2020), 4345–4356. http://dx.doi.org/10.3934/math.2020277

13. W. Shammakh, E. Mahmoud, B. Kashkari, Complex modified projective phase synchronization of nonlinear chaotic frameworks with complex variables, *Alex. Eng. J.*, **59** (2020), 1265–1273. http://dx.doi.org/10.1016/j.aej.2020.02.019

14. M. Aghababa, Finite-time chaos control and synchronization of fractional-order nonautonomous chaotic (hyperchaotic) systems using fractional nonsingular terminal sliding mode technique, *Nonlinear Dyn.*, **69** (2012), 247–261. http://dx.doi.org/10.1007/s11071-011-0261-6

15. C. Li, J. Zhang, Synchronisation of a fractional-order chaotic system using finite-time input-to-state stability, *Int. J. Syst. Sci.*, **47** (2016), 2440–2448. http://dx.doi.org/10.1080/00207721.2014.998741

16. R. Behinfaraz, M. Badamchizadeh, Optimal synchronization of two different in-commensurate fractional-order chaotic systems with fractional cost function, *Complexity*, **21** (2016), 401–416. http://dx.doi.org/10.1002/cplx.21754

17. M. Tavazoei, M. Haeri, Synchronization of chaotic fractional-order systems via active sliding mode controller, *Physica A*, **387** (2008), 57–70. http://dx.doi.org/10.1016/j.physa.2007.08.039

18. X. Zhang, Z. Li, D. Chang, Dynamics, circuit simulation and synchronization of a new three-dimensional fractional-order chaotic system, *AEU-Int. J. Electron. C.*, **82** (2017), 435–445. http://dx.doi.org/10.1016/j.aeue.2017.10.020

19. S. Wang, S. Zheng, L. Cui, Finite-time projective synchronization and parameter identification of fractional-order complex networks with unknown external disturbances, *Fractal Fract.*, **6** (2022), 298. http://dx.doi.org/10.3390/fractalfract6060298

20. X. Liao, On the global basin of attraction and positively invariant set for the Lorenz chaotic system and its application in chaos control and synchronization, *Sci. China Ser. E*, **34** (2004), 1404–1419.

21. P. Wang, Y. Zhang, S. Tan, L. Wan, Explicit ultimate bound sets of a new hyper-chaotic system and its application in estimating the Hausdorff dimension, *Nonlinear Dyn.*, **74** (2013), 133–142. http://dx.doi.org/10.1007/s11071-013-0953-1

22. J. Jian, Z. Zhao, New estimations for ultimate boundary and synchronization control for a disk dynamo system, *Nonlinear Anal.-Hybri.*, **9** (2013), 56–66. http://dx.doi.org/10.1016/j.nahs.2012.12.002

23. J. Wang, Q. Zhang, Z. Chen, H. Li, Ultimate bound of a 3D chaotic system and its application in chaos synchronization, *Abstr. Appl. Anal.*, **2014** (2014), 781594. http://dx.doi.org/10.1155/2014/781594

24. X. Zhang, Dynamics of a class of nonautonomous Lorenz-type systems, *Int. J. Bifurcat. Chaos*, **26** (2016), 1650208. http://dx.doi.org/10.1142/S0218127416502084

25. F. Chien, A. Roy Chowdhury, H. Saberi Nik, Competitive modes and estimation of ultimate bound sets for a chaotic dynamical financial system, *Nonlinear Dyn.*, **106** (2021), 3601–3614. http://dx.doi.org/10.1007/s11071-021-06945-8

26. F. Chien, M. Inc, H. Yosefzade, H. Saberi Nik, Predicting the chaos and solution bounds in a complex dynamical system, *Chaos Soliton. Fract.*, **153** (2021), 111474. http://dx.doi.org/10.1016/j.chaos.2021.111474

27. G. Leonov, A. Bunin, N. Koksch, Attraktorlokalisierung des Lorenz-Systems, *ZAMM*, **67** (1987), 649–656. http://dx.doi.org/10.1002/zamm.19870671215

28. G. Leonov, Lyapunov dimension formulas for Henon and Lorenz attractors, *St Petersb. Math. J.*, **13** (2001), 1–12.

29. G. Leonov, Lyapunov functions in the attractors dimension theory, *J. Appl. Math. Mech.*, **76** (2012), 129–141. http://dx.doi.org/10.1016/j.jappmathmech.2012.05.002

30. P. Swinnerton-Dyer, Bounds for trajectories of the Lorenz equations:an illustration of how to choose Liapunov functions, *Phys. Lett. A*, **281** (2001), 161–167. http://dx.doi.org/10.1016/S0375-9601(01)00109-8

31. F. Zhang, X. Liao, Y. Chen, C. Mu, G. Zhang, On the dynamics of the chaotic general Lorenz system, *Int. J. Bifurcat. Chaos.*, **27** (2017), 1750075. http://dx.doi.org/10.1142/S0218127417500754

32. H. Saberi Nik, S. Effati, J. Saberi-Nadjafi, New ultimate bound sets and exponential finite-time synchronization for the complex Lorenz system, *J. Complexity*, **31** (2015), 715–730. http://dx.doi.org/10.1016/j.jco.2015.03.001

33. W. Gao, L. Yan, M. Saeedi, H. Saberi Nik, Ultimate bound estimation set and chaos synchronization for a financial risk system, *Math. Comput. Simulat.*, **154** (2018), 19–33. http://dx.doi.org/10.1016/j.matcom.2018.06.006

34. D. Kumar, S. Kumar, Ultimate numerical bound estimation of chaotic dynamical finance model, In: *Modern mathematical methods and high performance computing in science and technology*, Singapore: Springer, 2016, 71–81. http://dx.doi.org/10.1007/978-981-10-1454-3_6

35. J. Jian, K. Wu, B. Wang, Global Mittag-Leffler boundedness and synchronization for fractional-order chaotic systems, *Physica A*, **540** (2020), 123166. http://dx.doi.org/10.1016/j.physa.2019.123166

36. Q. Peng, J. Jian, Estimating the ultimate bounds and synchronization of fractional-order plasma chaotic systems, *Chaos Soliton. Fract.*, **150** (2021), 111072. http://dx.doi.org/10.1016/j.chaos.2021.111072

37. P. Wan, J. Jian, Global Mittag-Leffler boundedness for fractional-order complex-valued Cohen-Grossberg neural networks, *Neural Process. Lett.*, **49** (2019), 121–139. http://dx.doi.org/10.1007/s11063-018-9790-z

38. J. Jian, K. Wu, B. Wang, Global Mittag-Leffler boundedness of fractional-order fuzzy quaternion-valued neural networks with linear threshold neurons, *IEEE Trans. Fuzzy Syst.*, **29** (2021), 3154–3164. http://dx.doi.org/10.1109/TFUZZ.2020.3014659

39. G. Mahmoud, M. Al-Kashif, A. Farghaly, Chaotic and hyperchaotic attractors of a complex nonlinear system, *J. Phys. A: Math. Theor.*, **41** (2008), 055104. http://dx.doi.org/10.1088/1751-8113/41/5/055104

40. Q. Wei, X. Wang, X. Hu, Adaptive hybrid complex projective synchronization of chaotic complex system, *Trans. Inst. Meas. Control*, **36** (2014), 1093–1097. http://dx.doi.org/10.1177/0142331214534722

AIMS Press